This article has been accepted for publication in a future issue of this journal, but has not been fully edited. Content may change prior to final publication. Citation information: DOI 10.1109/JQE.2022.3145838, IEEE Journal of Quantum Electronics

Selectively-Grown Quantum Dot Active Region Lasers

Luke J. Mawst, *Fellow*, *IEEE*, Honghyuk Kim, Wei Wei, Disha Talreja, Thomas F. Kuech, *Fellow*, *IEEE*, Padma Gopalan

(Invited Paper)

***Abstract*—Nanopatterns formed by dense nanoscale (20-30nm diameter) block copolymer lithography and subsequent selective area MOVPE were utilized to realize room temperature operation of quantum dot (QD) active region laser diodes on InP substrates, by employing a carrier-injection layer adjacent to the QDs. Initial studies focused on InGaAs QDs grown on GaAs substrates, which exhibit relatively broad photoluminescence (PL) emission linewidths (FWHM~93meV at RT). Atomic force microscopy measurements reveal that a wide distribution of QD thickness variations correlates well to the observed broad PL linewidths, based on the simulated range of QD transitions. The fabricated edge-emitting devices on InP substrate exhibit lasing emission near 1.57~1.67 μm at room temperature with a threshold current density as low as 1.6 kA/cm^2 for 4mm-long devices. The observed dependency of device characteristics, such as threshold current density and lasing wavelength, on the cavity length and on the heat sink temperature suggests the dominant lasing transition energy corresponds to the QD excited state, except for the longest cavity length devices (L=4mm) which operate on the QD ground state transition near room temperature. We believe these data represent the only reports of lasers in this wavelength region employing QDs formed by diblock co-polymer lithography and selective area MOVPE growth. These data also suggest that QD height variations need to be further reduced, through MOVPE growth optimization, to achieve higher optical gain from the QD ground state transition.**

***Index Terms*— quantum dot lasers, nanofabrication, nanolithography, diode lasers,**

I. Introduction

Over the last decades, there is a great deal of literature regarding the development of quantum dot (QD) laser diodes (LD) realized through the Stranski-Krastanov (SK) growth mode. Such devices have demonstrated ultra-low threshold current densities and low device temperature sensitivity (i.e. high T_0, T_1) [1-13]. Driven by strain energy, quantum dots under the SK growth mode are spontaneously formed on top of an inevitable quantum well-like wetting layer. While the wetting layer underneath the QDs acts as a carrier reservoir for improving carrier collection into the QDs, it has also been identified as one of the factors leading to the low optical gain and high temperature sensitivity in the LD, as a result of the thermally activated carrier leakage out of the QDs into the wetting layers [14-16]. Thus, the electronic coupling between the QDs and wetting layer hinders the ability to achieve full three-dimensional QD carrier confinement. In addition, as the SK growth mode requires the use of a highly compressively-strained material as a driving force for the nucleation of the QD formation, careful optimization in the growth parameters are required, such as growth interruptions, to minimize the variation in the QD size and spatial distribution. By contrast, nanopatterning and selective area epitaxy (SAE) potentially offer a more controllable pathway for QD formation, allowing the QD size to be decoupled from the strain state of the material, leading to the formation of wetting layer-free QDs (i.e., full three-dimensional nano-confinement). Furthermore, unlike the wetting layer formed during the SK QD growth process, carrier injection layers can be strain- and thickness-engineered underneath the QDs so as to optimize the carrier collection efficiency of the QDs, providing greater flexibility than possible with an SK QD/wetting-layer structure. To date, many alternative approaches to the SK process have been successfully employed to fabricate such semiconductor-based nanostructures, including interferometric optical lithography, x-ray lithography, atomic force microscopy-based lithography, electron beam lithography, scanning tunnelling microscopy (STM) and self-organized anodic aluminium oxide membranes [17-23]. Among these reported nanopatterning methods, successful demonstration of QD laser active region at room temperature with relatively low threshold current density was reported only by e-beam lithography and selective area Metalorganic vapor phase epitaxy (SA-MOVPE) [20].

Manuscript received Dec 1, 2021. Authors gratefully acknowledge funding from Army research office (ARO) under W911NF2010185. PG acknowledges partial funding from NSF Award ID 2003891 for the phase behavior studies. We acknowledge the use of Wisconsin Centers for Nanoscale Technology, which is partially funded by NSF-MRSEC-1720415

L. J. Mawst is with University of Wisconsin-Madison, Madison, WI, 53706 (phone: 608-263-1705; e-mail: ljmawst@wisc.edu).

H. Kim was with University of Wisconsin-Madison. He is now with Lumileds, LLC (e-mail: honghyuk.kim@lumileds.com)

W. Wei was with University of Wisconsin-Madison. He is now with Intel Corporation.

D. Talreja was with University of Wisconsin-Madison (email: dishatalreja20001@gmail.com)

T.F. Kuech is with University of Wisconsin-Madison and National Science Foundation(email: tkuech@nsf.gov)

P. Gopalan is with University of Wisconsin-Madison. (e-mail: pgopalan@wisc.edu)

0018-9197 (c) 2021 IEEE. Personal use is permitted, but republication/redistribution requires IEEE permission. See http://www.ieee.org/publications_standards/publications/rights/index.html for more information.
Authorized licensed use limited to: University of Wisconsin. Downloaded on June 14,2022 at 16:03:42 UTC from IEEE Xplore. Restrictions apply.

This article has been accepted for publication in a future issue of this journal, but has not been fully edited. Content may change prior to final publication. Citation information: DOI 10.1109/JQE.2022.3145838, IEEE Journal of Quantum Electronics

However, in spite of the advantages of e-beam lithography, including precise areal control and high resolution, its lengthy fabrication time makes it less desirable for high-volume, large-scale device application. Many challenges also remain for the other nanopatterning techniques such as enhancing resolution, reducing processing time and simplifying processes for reduced cost in semiconductor device applications. An alternate approach to the QD formation by nanopatterning is the utilization of diblock copolymers combined with SA-MOVPE. Fabrication of various nanostructures using block copolymer thin films has been studied and is known as block copolymer (BCP) lithography [24-26]. Periodic dense arrays of a nanosized hole pattern can be achieved using cylinder-forming BCPs with a high degree of pore-size uniformity through spin-coating processes and pattern transfer procedures, which is applicable to large areas at low cost. Dapkus and co-workers [27], were the first to demonstrate very uniform (in height and lateral size) GaAs QD arrays with densities as high as ~10^{11} cm^{-2} by BCP lithography and SA-MOVPE. This initial work demonstrated that, in contrast with SK QD formation, lattice-matched QDs could be formed by the BCP and SA-MOVPE process. Later, employing BCP lithography and SA-MBE growth, compressively-strained InAs QDs were also demonstrated with similar high areal densities [28]. The first lasers demonstrated by the BCP lithography and SA-MOVPE process operated only at low temperatures (20K) and employed a lattice-matched InGaAsP (1.15Q) / $In_{0.53}Ga_{0.47}As$ / InGaAsP (1.15Q) (2/2/2nm) QD active region on InP substrate [29]. In this prior report, unlike what occurs for the SK growth mode, the formation of the QDs was completely decoupled with the strain energy. However, a continuing challenge for the selective QD growth includes reducing process-induced damages at the QD–substrate interface, which can act as non-radiative recombination centers and reduce the radiative efficiency of the QDs [30]. We have previously reported the use of CBr_4 in situ etching prior to the SA-MOVPE of the $In_{0.3}Ga_{0.7}As$ QD growths, which is believed to reduce the processing-related damage, evidenced by an enhanced luminescence intensity of the QD active region and an improved device performance at the operating temperature up to 80K [31]. However, while a narrow lateral size distribution was obtained by this approach, relatively broad emission spectrum was observed especially at room temperature. As a follow-up study, here we show that the origin of the broad emission linewidth from the selectively grown $In_{0.3}Ga_{0.7}As$ QDs is associated with the large variation of the QD heights, which was confirmed by atomic force microscopy and correlated with the photoluminescence spectrum using the resulting spread in calculated transition energies. In addition, we extend this work to realize lasers on InP with QD active regions formed by BCP lithography and SA-MOVPE growth. While SK QDs on GaAs have been been implemented extensively for high-performance diode lasers in the telecom O-band (λ~1.3 μm), similar levels of device performance have not been achieved for SK QD active region lasers on InP for accessing the C-band (λ~1.55 μm). QD lasers operating in this wavelength region are attractive for integration onto Si substrates for integrated photonics targeting mid-range communications. Recent studies on the heteroepitaxial MOVPE growth of ~1.55 μm emitting QD lasers on Si show great promise for such applications [32]. However, many challenges still exist for realizing high-density, uniform size, SK QDs formed on InP by MOVPE. In particular, the growth of isotropic InAs QDs on InP substrates for achieving the emission wavelength near the telecom C-band still remains quite challenging, primarily because of the smaller driving force for the nucleation of InAs QDs, stemming from the smaller lattice mismatch on InP [33]. This smaller lattice mismatch often results in broken quantum wire-like structures, which leads to spectral and polarization dependency of the modal gain on the cavity orientation of the edge emitting device structure [34-35]. On the other hand, QDs can be formed in a more controllable fashion, less dependent on lattice mismatch, by employing nanopatterns and SA-MOVPE, as the QD formation is decoupled from the strain state of the material. Here, we present studies regarding the luminescence and lasing characteristics of the QD active devices grown on InP substrates, where the active region is composed of a single stack of $In_{0.8}Ga_{0.2}As$ QDs formed through the BCP lithography and SA-MOVPE growth process.

II. InGaAs QDs on GaAs substrate

A. *Fabrication of $In_{0.3}Ga_{0.7}As$ QDs on GaAs substrate*

A single stacked GaAs/$In_{0.3}Ga_{0.7}As$/GaAs (3/3/3nm) QDs were formed using a nano-patterning and SA-MOVPE growth process described previously [31]. GaAs/$In_{0.3}Ga_{0.7}As$/GaAs (3/4/3nm) layered QDs were selectively grown on the SiNx template, which was defined by BCP lithography, as schematically shown in Fig. 1. Cylinder-forming PS-b-PMMA (PS: Polystyrene, PMMA: Poly (methyl methacrylate)) were used for BCP lithography, as described in previous studies [31, 36]. Prior to loading the sample into the MOVPE reactor for in situ etching and QD regrowth, a brief wet treatment using NH_4OH:DI = 1:10 mixture (in volume ratio) was carried out for 20 sec to remove the native oxide as well as any remaining organic contaminations. Afterwards, *in situ* etching using CBr_4 was carried out, prior to the layered QD growth, under AsH_3 for 90 second as reported in our previous study [31]. After the growth of the QDs, the wafer with QDs was removed from the MOVPE reactor, and SiNx template was successively etched by the 6:1 buffered oxide etchant, which was followed by MOVPE overgrowth of 100 nm thick GaAs for PL study. A small part of the wafer after the QD was taken and imaged by either scanning electron microscope (SEM) or atomic force microscope (AFM).

0018-9197 (c) 2021 IEEE. Personal use is permitted, but republication/redistribution requires IEEE permission. See http://www.ieee.org/publications_standards/publications/rights/index.html for more information.
Authorized licensed use limited to: University of Wisconsin. Downloaded on June 14,2022 at 16:03:42 UTC from IEEE Xplore. Restrictions apply.

This article has been accepted for publication in a future issue of this journal, but has not been fully edited. Content may change prior to final publication. Citation information: DOI 10.1109/JQE.2022.3145838, IEEE Journal of Quantum Electronics

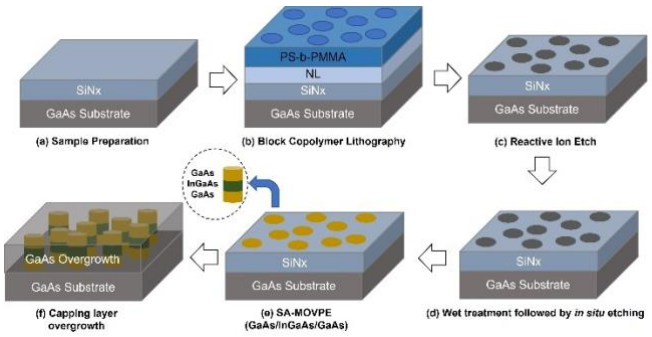

Fig. 1. Schematic representation of the nanopatterning and subsequent growth of the QDs on GaAs; (a) PECVD dielectric deposition; (b) BCP lithography; (c) RIE to transfer the nanopattern from BCP to SiNx using CF_4 plasma and subsequent BCP removal by O_2 plasma; (d) wet treatment and in-situ CBr_4 etching; (e) SAE in the MOVPE reactor; (f) Capping layer regrowth by MOVPE

B. *Structural and Optical Characteristics*

Fig. 2 shows the top view SEM image of the QDs taken after SiNx hardmask removal. The QD lateral size distribution within a limited area (400×400 nm^2). The measured distribution is fitted in normal distribution curve with a mean value of 25.6 nm and the standard deviation of 1.27 nm. In addition, the areal QD density was estimated to be near 8×10^{10} cm^{-2}. This lateral QD size distribution is as narrow as those from high performance QD lasers [37]. In addition, the areal QD density was comparable with those grown by optimized SK growth mode [38].

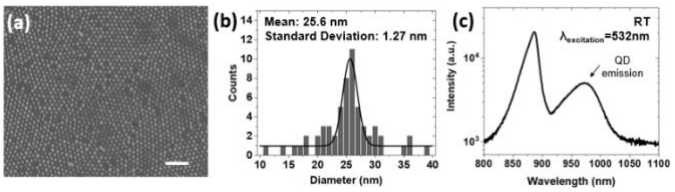

Fig. 2. (a) Top view SEM images of the GaAs/$In_{0.3}Ga_{0.7}As$/GaAs QDs grown after in situ etching (~3nm of etching) (scale bar:200nm), (b) their corresponding QD size distribution and (c) photoluminescence spectrum measured at room temperature

Fig. 3 (a), (b), and (c) shows an atomic force microscope image of the grown $In_{0.3}Ga_{0.7}As$ QDs, height distribution, and distribution of simulated emission wavelength for each QD with varying height, which was calculated by nextnano3 software package [39]. The distribution of the simulated emission wavelengths and the subsequent fitting to the normal distribution reveals a good correlation with the measured FWHM in the PL measurement (100meV by simulation vs. 93meV by PL measurement). This PL FWHM is still significantly higher than those of the state-of-art QDs grown by MBE under the SK growth mode (~23.8meV) [40]. The observed inhomogeneous broadening in the PL FWHM is believed to be originating from local variation of the growth rate in each opening during the selective area epitaxy. Therefore, this result suggests a further optimization in the selective growth conditions are necessary in order to achieve a narrow emission linewidth.

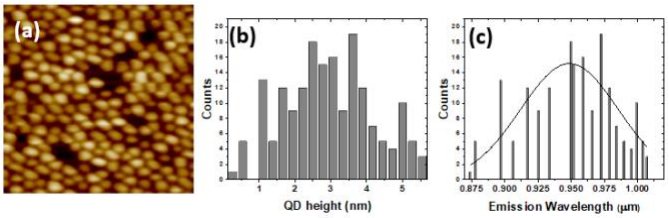

Fig. 3. (a) 500×500 nm^2 atomic force microscopic image; (b) Estimated $In_{0.3}Ga_{0.7}As$ QD height distribution from AFM measurement; and (c) simulated emission wavelength distribution (histogram) from the QD height distribution from AFM measurements and the subsequent fit (solid line).

Laser diodes employing the QDs which have the characteristics shown in Figure 3, were reported in our previous studies [31], where the devices operate up to 80K with a threshold current density, J_{th} of 385A/cm^2. However, at room temperature, lasing originating from the $In_{0.3}Ga_{0.7}As$ QD transitions was not observed, as shown in Fig. 4, which indicates low optical gain in the QD active region at room temperature as well as gain saturation, resulting in the laser emission (880nm) from the GaAs surrounding the QDs.

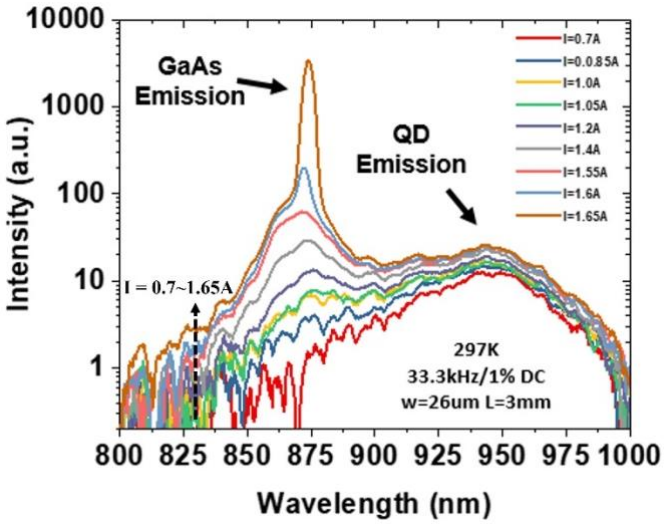

Fig. 4. Electroluminescence spectra at room temperature with varying injection current (L_{cav}=3mm)

In particular, the broad emission observed from the QD ensemble extends to the spectral region of GaAs emission as the current injection increases, indicating insufficient QD gain. It is anticipated that reducing the QD height variations will result in narrower spectral emission from the QDs and increased optical gain. These optimizations are the subject of future work. Furthermore, the results shown in Fig. 4, also suggests that it is necessary to improve the carrier capture by QDs at room temperature since the lasing emission from the surrounding GaAs suggests a large amount of the carriers leak out of the InGaAs QDs into the surrounding GaAs. Our previous study has shown that the use of lower bandgap (InAs) QDs together with a carrier collecting layer, which is placed adjacent to the QDs, helps improve carrier injection into the QDs, leading to lasing at room temperature [41]. These structures consist of a single stack 1.5 nm-thick InAs QD active region, which emits near 980nm, together with a 4 nm $In_{0.1}Ga_{0.9}As$ carrier collecting layer adjacent to the InAs QDs.

0018-9197 (c) 2021 IEEE. Personal use is permitted, but republication/redistribution requires IEEE permission. See http://www.ieee.org/publications_standards/publications/rights/index.html for more information.
Authorized licensed use limited to: University of Wisconsin. Downloaded on June 14,2022 at 16:03:42 UTC from IEEE Xplore. Restrictions apply.

This article has been accepted for publication in a future issue of this journal, but has not been fully edited. Content may change prior to final publication. Citation information: DOI 10.1109/JQE.2022.3145838, IEEE Journal of Quantum Electronics

These studies also indicated that for thicknesses greater than ~2nm strain relaxation occurs for the selectively grown InAs QDs on GaAs substrate, which results in the degradation in the luminescent properties. While lasing at room temperature was achieved by employing in situ etching prior to QD growth, InAs based QDs, and a carrier collecting layer underneath the QDs, the J_{th} observed was still relatively high (6.8kA/cm^2) , in comparison to those of SK QD lasers. One possible explanation for the high J_{th} value is that the approach employing selective area epitaxy and regrowth for the upper device structure inevitably involves exposing the uncapped QDs to the external environment outside of the growth chamber, which can lead to surface contamination and formation of surface defect states. In addition, the GaAs based material system is known to possess significantly higher surface recombination velocities (~100 times), than those of InP [42-43]. Therefore, our further investigation to realize lower threshold current density lasers focussed on the selective growth of QDs on InP substrates, as discussed in the following section.

III. InGaAs QDs on InP substrates

A. Fabrication of $In_{0.8}Ga_{0.2}As$ QDs on InP substrate

A single stack $In_{0.8}Ga_{0.2}As$ QD active region laser was selectively grown on InP substrates in the similar manner to those of GaAs substrate, as schematically shown in Fig. 5 [31]. Trimethyl-indium (TMIn), trimethyl-gallium (TMGa), trimethyl-aluminium (TMAl), arsine (AsH_3) and phosphine (PH_3) were used as In, Ga, Al, As, and P precursors, respectively.

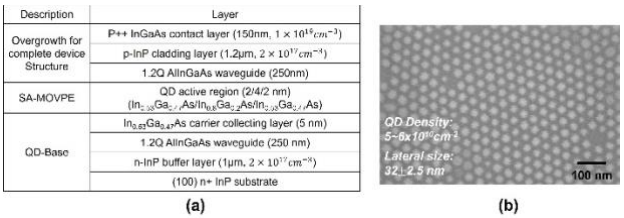

Fig. 5. (a) Schematic diagram of the complete laser structure and multi-step growth sequence, (b) Top-view scanning electron microscopic image taken after the selective area epitaxy for QD growth and the subsequent removal of SiNx hardmask

in situ etching by CBr_4 was performed prior to the growth of the layered $In_{0.53}Ga_{0.47}As$ / $In_{0.8}Ga_{0.2}As$ / $In_{0.53}Ga_{0.47}As$ / InP (2/4/2/2nm) as reported elsewhere [44]. The base structure consists of an AlInGaAs (λ~1.1μm) lattice-matched waveguide and a $In_{0.53}Ga_{0.47}$ carrier collecting layer (~5nm), which is believed to help improve the carrier injection into the QDs. On top of the carrier collecting layer, a thin sacrificial InP layer (~2nm) was also grown. Prior studies have shown that in situ etching using CBr_4 leads to a higher selectivity for InP than InGaAs or AlInAs [44]. Based on this etching selectivity, A thin InP sacrificial layer was removed by in situ etching prior to the SA-MOVPE for the QD growth and subsequent regrowth for the complete device structure. The areal density of the selectively grown QDs was as high as 5~6×10^{10}cm^{-2} and the average QD diameter of 32 nm, as shown in Figure 5.

B. Optical characteristics of the laser structure

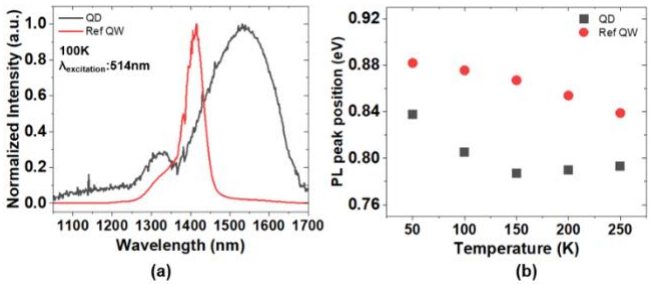

Fig. 6. (a) PL spectra at 100K from the complete QD laser structure where the p++ InGaAs contact layer is removed. PL spectrum from the reference QW sample (Ref QW) is shown, where no QD growth was carried out, and (b) PL peak position shift with varying measurement temperature

Prior to laser fabrication, we characterized the structure shown in Fig. 5 using variable temperature photoluminescence measurements. Fig. 6 shows the PL spectrum of the complete QD laser structure (with p++ InGaAs contact layer removed) as well as a control structure where no selective QD growth was carried out. The peak near 1400nm from the ref QW corresponds carrier recombination in the 5nm thick InGaAs carrier collecting layer. By contrast, broad (FWHM ~ 108 meV) spectral emission near 1550nm is observed from the QD laser structure, which is attributed to the variation in the QD height, as discussed above regarding the QDs on GaAs. The secondary spectral feature appearing near 1300nm is possibly attributed to the excited state of the carrier collecting/QD coupled structure, or an interfacial transition layer. As the measurement temperature increases, the ref QW sample exhibited a gradual decrease in the transition energy as evidenced by PL peak position shown in Fig. 6 (b), while the QD sample shows insensitivity in the transition energy above 150K, which is ascribed to carrier localization effects.

C. Electrical and Optical Characteristics of $In_{0.8}Ga_{0.2}As$ QD Lasers

Using the material shown in Figure 5, broad-area ridge-guide lasers are fabricated and characterized under short pulsed current operation. Shown in Fig. 7. are the output power vs. input current characteristics under pulsed operation (pulse width:200nsec, duty cycle: 0.5%) for the devices with varying cavity length at the heat sink temperature from 10 to 50°C.

Long cavity length devices, L=4mm, exhibit low threshold current densities (J_{th}~1.6kA/cm^2) at a heatsink temperature of 10°C. As shown in Figure 7, the threshold current density increases dramatically for shorter cavity length devices, reflecting the low modal optical gain associated with the QD ground state transition of the single QD layer active region. Therefore, multi-stacked QD layers will be necessary to achieve a lower J_{th} with a shorter cavity length. This could possibly be realized by SAE of multi stacked layers with a thicker SiN_x template, which remains as a subject of our ongoing study. Also shown in Figure 7, the characteristic temperature coefficient values for the threshold current density (T_0) are also

0018-9197 (c) 2021 IEEE. Personal use is permitted, but republication/redistribution requires IEEE permission. See http://www.ieee.org/publications_standards/publications/rights/index.html for more information.
Authorized licensed use limited to: University of Wisconsin. Downloaded on June 14,2022 at 16:03:42 UTC from IEEE Xplore. Restrictions apply.

This article has been accepted for publication in a future issue of this journal, but has not been fully edited. Content may change prior to final publication. Citation information: DOI 10.1109/JQE.2022.3145838, IEEE Journal of Quantum Electronics

significantly lower for the long cavity length devices. Similar trends were reported previously from devices employing a single layer of InAs QDs surrounded by an InGaAs QW grown on GaAs substrate [7]. Such behavior was ascribed to the larger density of excited states (ES) for the QDs, leading to a higher J_{th} and higher T_0 values at shorter cavity lengths [7]. Nevertheless, the J_{th} values reported here are comparable with that from the SK-mode grown single-layer InAs QD lasers emitting the similar wavelength (3.5 kA/cm^2, pulsed (this work) vs. 2.75 kA/cm^2, CW [52]) at the same cavity length (L=2mm), as shown in Table 1.

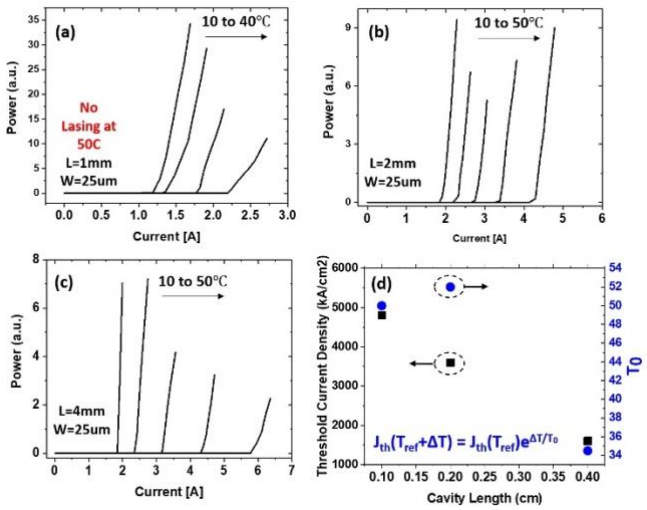

Fig. 7 (a) Output power vs. current (PI) for 1mm-long QD device where no lasing was observed at 50°C, (b) Output power vs. current (PI) for 2mm-long QD device, (c) Output power vs. current (PI) for 4mm-long QD device, (d) summary of threshold current density at heat sink temperature of 10°C and the characteristic temperature as a function of cavity length

Presented in Fig. 8 (a) is the EL spectra from the 4mm-long QD device measured at I=~1.3I_{th} while varying heat sink temperature from 5 to 50°C. At 15~20°C, the 4mm-long devices exhibit a sudden drop in the lasing wavelength from 1.67μm to 1.59μm, most likely due to a switch from the QD ground state transition to an excited state. The calculated transition energies at 283K of the target structure, shown in Fig. 6. (b), correspond to GS: 0.717eV (1.73 μm) and the ES: 0.761 eV (1.63 μm), which was carried out by constructing the 3-dimensional QD structure using a commercial Schrodinger/Poisson solver [39]. In order to further verify the origin of the discrepancy between simulated and observed wavelength, a further investigation involving either tunneling electron microscopy or atom probe tomography is necessary to better quantify the compositional and shape profiles of the QDs. Fig. 7 (c) shows the variation in the peak lasing wavelengths from the 2-mm long and 4mm-long QD devices, as well as a reference 3-QW laser (3x $In_{0.65}Ga_{0.35}As$/AlInGaAs (7.5/15 nm) emitting at a similar lasing wavelength. In contrast to the long cavity length devices, the shorter 2mm-long QD devices do not exhibit ground state emission, since lasing occurs at 1.56μm, which close to that for the simulated excited state (ES) transition. As evident from Figure 8 (b), a relatively low sensitivity in the lasing wavelength to temperature is observed, particularly for operation on the excited state transition. Such

TABLE I
COMPARISON OF SELECTED QD ACTIVE LASERS

Ref	Number of QD Stacks	J_{th} (Temp)	λ_{lasing} (μm)	T_0 (~RT) (K)
45	5	380A/cm^2 (23°C, Pulsed)	1.63	50
46	7	~3.8kA/cm^2 (RT, Pulsed)	1.501	135
47	3	190A/cm^2 (27°C, Pulsed)	1.59	25~55
48	1	9.4kA/cm^2 (2°C, Pulsed)	1.67	61
49	6	1.4kA/cm^2(20°C, CW)	1.5	56
50	6	~6kA/cm^2(27°C, Pulsed)	1.55	70
51	6	3.7kA/cm2 (20°C, Pulsed)	1.545	144
52	1	2.75 kA/cm^2 (RT, CW)	1.68	N/A
This work	1	1.6 kA/cm2 (10°C, Pulsed)	1.67	34

weak temperature dependency in the lasing wavelength with temperature (0.09nm/K) was reported previously from a single-layer SK InAs QD laser on InP substrate emitting near 1.7 μm [50].

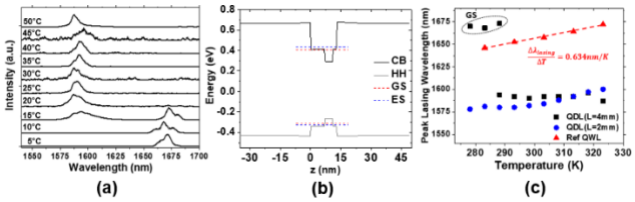

Fig. 8 (a) Lasing spectrum from 4mm-long device, (b) calculated band diagram and transition energy at 283K where the conduction band edge of the conduction band, heavy hole band are denoted as CB and HH respectively, and (c) summary of peak lasing wavelength as a function of heat sink temperature

For reference, a conventional 3-QW laser (3x $In_{0.65}Ga_{0.35}As$/AlInGaAs (7.5/15 nm)) emitting at a similar wavelength exhibits a monotonic increase in the lasing wavelength with temperature coefficient ($\Delta\lambda$lasing/ΔT) of 0.634 nm/K. This observation suggests that an additional optimization in the active region heterostructure is necessary to improve the carrier injection efficiency into the GS, which can be possibly realized by employing tunnel injection scheme [53]. It is noteworthy that the overlapping spectral features between QD excited state and the electronic state of the carrier collection layer make it difficult to determine the exact origin of the higher energy laser emission. However, the observed low temperature sensitivity in the laser wavelength further substantiates that the higher energy spectral features correlate with that expected from the QD state transition. Spectral gain measurement and loss extraction via segmented contact method are the subject of our ongoing work [29], in order to further elucidate the optical gain properties of the QD GS and ES.

IV. CONCLUSION

We have shown the luminescent properties of the selectively grown InGaAs based QDs on either GaAs or InP substrates. $In_{0.3}Ga_{0.7}As$ QDs on GaAs substrates exhibit a broad PL emission which corresponds to the inhomogeneous broadening

0018-9197 (c) 2021 IEEE. Personal use is permitted, but republication/redistribution requires IEEE permission. See http://www.ieee.org/publications_standards/publications/rights/index.html for more information.
Authorized licensed use limited to: University of Wisconsin. Downloaded on June 14,2022 at 16:03:42 UTC from IEEE Xplore. Restrictions apply.

This article has been accepted for publication in a future issue of this journal, but has not been fully edited. Content may change prior to final publication. Citation information: DOI 10.1109/JQE.2022.3145838, IEEE Journal of Quantum Electronics

resulting from the large QD height distribution. Even with chemical pre-growth treatment, using CBr_4 in situ etching, and the presence of a carrier collecting layer adjacent to the QD active region, the selectively grown QD lasers on GaAs substrate exhibit high threshold current density (6.8kA/cm^2 at RT), relative to those of conventional SK QD lasers, which is most likely associated with the high surface recombination that is exacerbated during the subsequent fabrication process during the QD formation. A similar QD formation process was implemented for realizing QD lasers on InP substrate, in order to exploit the inherent lower surface recombination velocities of such materials. Single layer $In_{0.8}Ga_{0.2}As$ QD active region laser devices exhibit a dramatic reduction in J_{th}, as well as a sudden drop in T_0 value, with increasing cavity length. Threshold current densities as low as 1.6 kA/cm^2 are observed for 4mm cavity length devices, which is comparable to values reported for SK QD lasers in the wavelength region. The much lower J_{th} in comparison to that of the QD active devices formed on GaAs substrates is attributed to the lower surface recombination for InP based materials. The lasing wavelength was observed to be insensitive to temperature in comparison with the reference QW device, although the laser emission corresponded to an exited state transition of the QD active region. Further optimization in the device structure and QD selective growth conditions is necessary to achieve higher modal gain, which would allow ground state emission from reduced cavity length devices.

REFERENCES

[1] M. Asada, Y. Miyamoto, and Y. Suematsu, “Gain and the threshold of three-dimensional quantum-box lasers,” IEEE J. Quantum Electron., vol. 22, no. 9, pp. 1915–1921, 1986.

[2] N. N. Ledentsov, “Long-wavelength quantum-dot lasers on GaAs substrates: from media to device concepts,” IEEE J. Sel. Top. Quantum Electron., vol. 8, no. 5, pp. 1015–1024, 2002

[3] D. G. Deppe, K. Shavritranuruk, G. Ozgur, H. Chen, and S. Freisem, “Quantum dot laser diode with low threshold and low internal loss,” Electron. Lett., vol. 45, no. 1, p. 54, 2009

[4] L. Seravalli, P. Frigeri, G. Trevisi, and S. Franchi, “1.59μm room temperature emission from metamorphic InAs⁄InGaAs quantum dots grown on GaAs substrates,” Appl. Phys. Lett., vol. 92, no. 21, p. 213104, 2008

[5] H. Y. Liu, Y. Qiu, C. Y. Jin, T. Walther, and A. G. Cullis, “1.55μm InAs quantum dots grown on a GaAs substrate using a GaAsSb metamorphic buffer layer,” Appl. Phys. Lett., vol. 92, no. 11, p. 111906, 2008

[6] R. Mirin, A. Gossard, and J. Bowers, “Room temperature lasing from InGaAs quantum dots,” Electron. Lett., vol. 32, no. 18, p. 1732, 1996

[7] G. T. Liu, A. Stintz, H. Li, K. J. Malloy, L. F. Lester, "Extremely low room-temperature threshold current density diode lasers using InAs dots in InGaAs quantum well", Electron. Lett., vol. 35, pp. 1163-1165, 1999

[8] G. Park, D. L. Huffaker, Z. Zou, O. B. Shchekin, D. G. Deppe, " Temperature dependence of lasing characteristics for long wavelength (1.3 μm) GaAs-based quantum dot lasers ", IEEE Photon. Technol. Lett., vol. 11, pp. 301-303, 1999.

[9] H. Shoji, K. Mukai, N. Ohtsuka, M. Sugawara, T. Uchida, and H. Ishikawa, “Lasing at three-dimensionally quantum-confined sublevel of self-organized $In_{0.5}Ga_{0.5}As$ quantum dots by current injection,” IEEE Photonics Technol. Lett., vol. 7, no. 12, pp. 1385–1387, 1995

[10] Y. Qiu, P. Gogna, S. Forouhar, A. Stintz, and L. F. Lester, “High-performance InAs quantum-dot lasers near 1.3 μm,” Appl. Phys. Lett., vol. 79, no. 22, pp. 3570–3572, 2001

[11] H.-Y. Liu, B. Xu, Y.-Q. Wei, D. Ding, J.-J. Qian, Q. Han, J.-B. Liang, Z.-G. Wang, "High-power and long-lifetime InAs/GaAs quantum-dot laser at 1080 nm", Appl. Phys. Lett., vol. 79, pp. 2868-2870, 2001.

[12] F. Klopf, J. P. Reithmaier, and A. Forchel, “Highly efficient GaInAs/(Al)GaAs quantum-dot lasers based on a single active layer versus 980 nm high-power quantum-well lasers,” Appl. Phys. Lett., vol. 77, no. 10, pp. 1419–1421, 2000

[13] J. Tatebayashi, N. Hatori, H. Kakuma, H. Ebe, H. Sudo, A. Kuramata, Y. Nakata, M. Sugawara and Y. Arakawa, “Low threshold current operation of self-assembled InAs⁄GaAs quantum dot lasers by metal organic chemicalvapour deposition,” Electron. Lett., vol. 39, no. 15, p. 1130, 2003

[14] D. R. Matthews, H. D. Summers, P. M. Smowton, and M. Hopkinson, “Experimental investigation of the effect of wetting-layer states on the gain–current characteristic of quantum-dot lasers,” Appl. Phys. Lett., vol. 81, no. 26, pp. 4904–4906, 2002

[15] D. Colombo et al., “Efficient room temperature carrier trapping in quantum dots by tailoring the wetting layer,” J. Appl. Phys., vol. 94, no. 10, pp. 6513–6517, 2003

[16] Heitz, R., et al. "Excited states and energy relaxation in stacked InAs/GaAs quantum dots." Phys. Rev. B 57, 9050, 1998.

[17] S. Birudavolu et al., “Selective area growth of InAs quantum dots formed on a patterned GaAs substrate,” Appl. Phys. Lett., vol. 85, no. 12, pp. 2337–2339, 2004

[18] Warren, A. C., et al. " “Fabrication of sub-100-nm linewidth periodic structures for study of quantum effects from interference and confinement in Si inversion layers,” J. Vac. Sci. Technol. B Microelectron. Nanometer Struct. Process. Meas. Phenom., vol. 4, no. 1, p. 365, 1986

[19] S. Lüscher et al., “Quantum wires and quantum dots defined by lithography with an atomic force microscope,” Microelectronics, vol. 33, no. 4, pp. 319–321, 2002

[20] V. C. Elarde, A. C. Bryce, and J. J. Coleman, “High performance laser with nanopatterned active layer by selective area epitaxy,” Electron. Lett., vol. 41, no. 20, p. 1122, 2005

[21] Y. Nakamura, N. Ikeda, S. Ohkouchi, Y. Sugimoto, H. Nakamura, and K. Asakawa, “Regular array of InGaAs quantum dots with 100-nm-periodicity formed on patterned GaAs substrates,” Physica E Low Dimens. Syst. Nanostruct., vol. 21, no. 2–4, pp. 551–554, 2004

[22] H. S. Lee et al., “Selective area wavelength tuning of InAs/GaAs quantum dots obtained by TiO2 and SiO2 layer patterning,” Appl. Phys. Lett., vol. 94, no. 16, p. 161906, 2009

[23] S. Kohmoto, H. Nakamura, T. Ishikawa, and K. Asakawa, “Site-controlled self-organization of individual InAs quantum dots by scanning tunneling probe-assisted nanolithography,” Appl. Phys. Lett., vol. 75, no. 22, pp. 3488–3490, 1999

[24] M. Park, C. Harrison, P. M. Chaikin, R. A. Register, and D. H. Adamson, “Block copolymer lithography: Periodic arrays of ~10^{11} holes in 1 square centimeter,” Science, vol. 276, no. 5317, pp. 1401–1404, 1997

[25] G. Liu, J. Ding, T. Hashimoto, K. Kimishima, F. M. Winnik, and S. Nigam, “Thin films with densely, regularly packed nanochannels: Preparation, characterization, and applications,” Chem. Mater., vol. 11, no. 8, pp. 2233–2240, 1999

[26] A. Sidorenko, I. Tokarev, S. Minko, and M. Stamm, “Ordered reactive nanomembranes/nanotemplates from thin films of block copolymer supramolecular assembly,” J. Am. Chem. Soc., vol. 125, no. 40, pp. 12211–12216, 2003

[27] R. R. Li et al., “Dense arrays of ordered GaAs nanostructures by selective area growth on substrates patterned by block copolymer lithography,” Appl. Phys. Lett., vol. 76, no. 13, pp. 1689–1691, 2000

[28] A. Alizadeh et al., “Epitaxial growth of 20 nm InAs and GaAs quantum dots on GaAs through block copolymer templated SiO2 masks,” J. Appl. Phys., vol. 105, no. 5, p. 054305, 2009

[29] L. Mawst, G. Tsvid, P. Dudley, J. Kirch, J. H. Park, and N. Kim, “Radiative efficiency of MOCVD grown QD lasers,” in Physics and Simulation of Optoelectronic Devices XVIII, 2010

[30] T. F. Kuech and L. J. Mawst, “Nanofabrication of III–V semiconductors employing diblock copolymer lithography,” J. Phys. D Appl. Phys., vol. 43, no. 18, p. 183001, 2010.

[31] H. Kim et al., “Selective growth of strained (In)GaAs quantum dots on GaAs substrates employing diblock copolymer lithography nanopatterning,” J. Cryst. Growth, vol. 465, pp. 48–54, 2017

[32] S. Zhu, B. Shi, Q. Li, and K. M. Lau, “1.5μm quantum-dot diode lasers directly grown on CMOS-standard (001) silicon,” Appl. Phys. Lett., vol. 113, no. 22, p. 221103, 2018

[33] C. Gilfert, V. Ivanov, N. Oehl, M. Yacob, and J. P. Reithmaier, “High gain 1.55 μm diode lasers based on InAs quantum dot like active regions,” Appl. Phys. Lett., vol. 98, no. 20, p. 201102, 2011

[34] A. A. Ukhanov et al., “Orientation dependence of the optical properties in InAs quantum-dash lasers on InP,” Appl. Phys. Lett., vol. 81, no. 6, pp. 981–983, 2002

0018-9197 (c) 2021 IEEE. Personal use is permitted, but republication/redistribution requires IEEE permission. See http://www.ieee.org/publications_standards/publications/rights/index.html for more information.
Authorized licensed use limited to: University of Wisconsin. Downloaded on June 14,2022 at 16:03:42 UTC from IEEE Xplore. Restrictions apply.

This article has been accepted for publication in a future issue of this journal, but has not been fully edited. Content may change prior to final publication. Citation information: DOI 10.1109/JQE.2022.3145838, IEEE Journal of Quantum Electronics

[35] B. Dong et al., "Influence of the polarization anisotropy on the linewidth enhancement factor and reflection sensitivity of 1.55-μm InP-based InAs quantum dash lasers," Appl. Phys. Lett., vol. 115, no. 9, p. 091101, 2019
[36] C.-C. Liu, "Nanoscale selective growth and optical characteristics of quantum dots on III-V substrates prepared by diblock copolymer nanopatterning," J. Nanophotonics, vol. 3, no. 1, p. 031604, 2009
[37] M. V. Maximov et al., "High-power continuous-wave operation of a InGaAs/AlGaAs quantum dot laser," J. Appl. Phys., vol. 83, no. 10, pp. 5561–5563, 1998
[38] L. F. Lester et al., "Optical characteristics of 1.24-μm InAs quantum-dot laser diodes," IEEE Photonics Technol. Lett., vol. 11, no. 8, pp. 931–933, 1999
[39] The nextnano3 software package can be obtained from www.nextnano.de
[40] K. Nishi, K. Takemasa, M. Sugawara, and Y. Arakawa, "Development of quantum dot lasers for data-com and silicon photonics applications," IEEE J. Sel. Top. Quantum Electron., vol. 23, no. 6, pp. 1–7, 2017.
[41] H. Kim, W. Wei, T. F. Kuech, P. Gopalan, and L. J. Mawst, "Impact of InGaAs carrier collection quantum well on the performance of InAs QD active region lasers fabricated by diblock copolymer lithography and selective area epitaxy," Semicond. Sci. Technol., vol. 34, no. 2, p. 025012, 2019
[42] H. C. Casey Jr and E. Buehler, "Evidence for low surface recombination velocity onn-type InP," Appl. Phys. Lett., vol. 30, no. 5, pp. 247–249, 1977
[43] C. A. Hoffman, H. J. Gerritsen, and A. V. Nurmikko, "Study of surface recombination in GaAs and InP by picosecond optical techniques," J. Appl. Phys., vol. 51, no. 3, pp. 1603–1604, 1980
[44] H. Kim, W. Wei, P. Gopalan, T. F. Kuech, L. J. Mawst, "In0.8Ga0.2As QD active region (λ~1.65μm) laser diodes grown by block copolymer lithography and selective area OMVPE", 19th International Conference on Crystal Growth and Epitaxy (ICCGE-19) and 19th US Biennial Workshop on Organometallic Vapor Phase Epitaxy (OMVPE-19), Keystone Resort, Keystone, Colorado, USA, Jul 28 – Aug 2, 2019
[45] H. Saito, K. Nishi, and S. Sugou, "Ground-state lasing at room temperature in long-wavelength InAs quantum-dot lasers on InP(311)B substrates," Appl. Phys. Lett., vol. 78, no. 3, pp. 267–269, 2001
[46] J. S. Kim et al., "Room-temperature operation of InP-based InAs quantum dot laser," IEEE Photonics Technol. Lett., vol. 16, no. 7, pp. 1607–1609, 2004
[47] P. Caroff et al., "High-gain and low-threshold InAs quantum-dot lasers on InP," Appl. Phys. Lett., vol. 87, no. 24, p. 243107, 2005
[48] Y. Qiu, D. Uhl, R. Chacon, and R. Q. Yang, "Lasing characteristics of InAs quantum-dot lasers on (001) InP substrate," Appl. Phys. Lett., vol. 83, no. 9, pp. 1704–1706, 2003
[49] F. Lelarge, B. Rousseau, B. Dagens, F. Poingt, F. Pommereau, and A. Accard, "Room temperature continuous-wave operation of buried ridge stripe lasers using InAs-InP (100) quantum dots as active core," IEEE Photonics Technol. Lett., vol. 17, no. 7, pp. 1369–1371, 2005
[50] D. Gready et al., "High Speed 1.55 μm InAs/InGaAlAs/InP Quantum Dot Lasers," IEEE Photonics Technol. Lett., vol. 26, no. 1, pp. 11–13, 2014
[51] A. Abdollahinia et al., "Temperature stability of static and dynamic properties of 1.55 μm quantum dot lasers," Opt. Express, vol. 26, no. 5, pp. 6056–6066, 2018
[52] J. Kotani et al., "First demonstration of single-layer InAs/InP (100) quantum-dot laser: continuous wave, room temperature, ground state," Electron. Lett., vol. 45, no. 25, p. 1317, 2009
[53] S. Bauer, V. Sichkovskyi, and J. P. Reithmaier, "Growth and optical characteristics of InAs quantum dot structures with tunnel injection quantum wells for 1.55 μm high-speed lasers," J. Cryst. Growth, vol. 491, pp. 20–25, 2018

Luke J. Mawst (M'88–SM'93–F'11) received the B.S. degree in engineering physics and the M.S. and Ph.D. degrees in electrical engineering all from the University of Illinois at Urbana-Champaign, Champaign, in 1982, 1984, and 1987, respectively. He joined TRW Inc., Redondo Beach, CA, in 1987, where he was a Senior Scientist in the TRW Research Center, engaged in the design and development of semiconductor lasers using MOCVD crystal growth. He is a Co-Inventor of the resonant optical waveguide (ROW) antiguided-array concept and has contributed to its development as a practical source of high coherent power. He developed a novel, single-mode edge-emitting laser structure; the ARROW laser, as a source for coupling high powers into single-mode optical fibers. He is currently a Professor in the Department of Electrical and Computer Engineering, University of Wisconsin–Madison, Madison, where he is involved in the development of novel III–V compound semiconductor device structures, including vertical-cavity surface emitters, active-photonic-crystal structures, dilute-nitride lasers, solar cells, lasers employing metamorphic buffer layers, and quantum cascade lasers. He is a Founder of Intraband LLC, a Madison-based developer of high-power quantum cascade lasers. He is the author or coauthor of more than 300 technical papers and holds 26 patents.

Honghyuk Kim received his BS at State University of New York at Stony Brook in 2012 and his Ph.D in electrical and computer engineering at University of Wisconsin-Madison in 2019. His research interests include epitaxy of III-V semiconductor of compound semiconductor as well as optoelectronic device physics. After working at Lawrence Berkeley National Laborary and Northwestern University as a postdoctoral scholar, he is now at Lumileds LLC working as a R&D development engineer..

Wei Wei received his Ph.D in Materials Science and Engineering at the University of Wisconsin-Madison in 2019. He is now at Intel.

Disha Talreja received her Ph.D in Materials Science and Engineering from Penn State University in 2020. She joined as a post-doctoral researcher in Electrical and Computer Engineering department at University of Wisconsin-Madison in 2020 where she worked on characterizing quantum dot lasers. She is currently doing her post-doc at University of Pennsylvania.

Thomas F. Kuech is an emeritus professor of the Chemical and Biological Engineering Department of the University of Wisconsin-Madison. He is a member of the National Academy of Engineering and is a Fellow of the American Physical Society, IEEE, MRS and AAAS. He has served as an executive officer in several professional societies, such as president of the American Association for Crystal Growth, as well as organizing and chairing several major national and international conferences. He has been involved in the study of the chemical and physical processes underlying the synthesis of semiconductor materials and structures.

Padma Gopalan received her Ph.D in Chemistry from Cornell University in 2001, on liquid crystalline block copolymers and their self-assembly. She conducted her postdoctoral work in Lucent Technologies, Bell Laboratories, on organic electro-optic modulators. She is currently a Professor in the Department of Materials Science and Eng. at the University of Wisconsin-Madison, and holds an affiliate appointment in the Departments of Chemistry and Chemical and Biological Engineering. She is an expert in the synthesis of self-assembling block copolymers, and polymer brushes, their self-assembly in thin-films and their applications in nano-patterning. She developed the methodology to vertically align block copolymer domains in thin-films using a universal coating chemistry that can be applied to substrates of varied compositions. She is the recipient of NSF-CAREER in 2005. From 2012 – 2015 she directed the NSF funded NSEC center at UW-Madison. She is the recipient of the Romnes Faculty Fellowship from Wisconsin Alumni Research Foundation (2015), and the Vilas Distinguished Achievement Professorship (2015-2020) from UW-Madison. She was appointed to the prestigious position of a visiting Professor through the World Research Hub at Tokyo Institute of Technology, Japan, from 2018 to 2020.

0018-9197 (c) 2021 IEEE. Personal use is permitted, but republication/redistribution requires IEEE permission. See http://www.ieee.org/publications_standards/publications/rights/index.html for more information.
Authorized licensed use limited to: University of Wisconsin. Downloaded on June 14,2022 at 16:03:42 UTC from IEEE Xplore. Restrictions apply.